THE JOURNAL OF BIOLOGICAL CHEMISTRY VOL. 285, NO. 20, pp. 15538–15547, May 14, 2010


# Increased E4 Activity in Mice Leads to Ubiquitin-containing Aggregates and Degeneration of Hypothalamic Neurons Resulting in Obesity*[S]

Received for publication, January 19, 2010, and in revised form, February 26, 2010 Published, JBC Papers in Press, February 26, 2010, DOI 10.1074/jbc.M110.105841

**Etsuo Susaki[‡§], Chie Kaneko-Oshikawa[‡§], Keishi Miyata[¶], Mitsuhisa Tabata[¶], Tetsuya Yamada[‖], Yuichi Oike[¶], Hideki Katagiri[‖], and Keiichi I. Nakayama[‡§1]**

*From the [‡]Department of Molecular and Cellular Biology, Medical Institute of Bioregulation, Kyushu University, 3-1-1 Maidashi, Higashi-ku, Fukuoka, Fukuoka 812-8582, [§]Core Research for Evolutional Science and Technology (CREST), Japan Science and Technology Agency, 4-1-8 Honcho, Kawaguchi, Saitama 332-0012, the [¶]Department of Molecular Genetics, Graduate School of Medical Sciences, Kumamoto University, 1-1-1 Honjo, Kumamoto 860-8556, and the [‖]Division of Advanced Therapeutics for Metabolic Diseases, Center for Translational and Advanced Animal Research, Tohoku University Graduate School of Medicine, 2-1 Seiryo-machi, Aoba-ku, Sendai 980-8575, Japan*

**Obesity has become a serious worldwide public health problem. Although neural degeneration in specific brain regions has been suggested to contribute to obesity phenotype in humans, a causal relationship between these two conditions has not been demonstrated experimentally. We now show that E4B (also known as UFD2a), a mammalian ubiquitin chain elongation factor (E4), induces the formation of intracellular aggregates positive for ubiquitin and the adaptor protein p62 when overexpressed in cultured cells or the brain. Mice transgenic for E4B manifested neural degeneration in association with aggregate formation, and they exhibited functional impairment specifically in a subset of hypothalamic neurons that regulate food intake and energy expenditure, resulting in development of hyperphagic obesity and related metabolic abnormalities. The neural pathology of E4B transgenic mice was similar to that of human neurodegenerative diseases associated with the formation of intracellular ubiquitin-positive deposits, indicating the existence of a link between such diseases and obesity and related metabolic disorders. Our findings thus provide experimental evidence for a role of hypothalamic neurodegeneration in obesity, and the E4B transgenic mouse should prove to be a useful animal model for studies of the relationship between neurodegenerative diseases and obesity.**

Insight into signaling pathways that control food intake and energy homeostasis in humans has been provided by animal models of obesity associated with diet manipulation, spontaneous mutation of key molecules, transgenesis, or gene knockout, or physical intervention (1). Such models have implicated hypothalamic neural circuits and related molecules such as leptin, insulin, agouti-related protein, neuropeptide Y, cocaine- and amphetamine-regulated transcript protein, and pro-opiomelanocortin (POMC)[2] in this regulatory system (2–4). In addition to shedding light on the mechanisms of human obesity and related disorders, these model animals have contributed to the development of new drugs for the treatment of this increasingly prevalent threat to public health. Establishment of additional animal models for obesity based on newly identified pathogenetic mechanisms may thus provide further key information for potential therapeutic intervention.

The ubiquitin-proteasome system plays a pivotal role in many cellular processes (5, 6). The ubiquitylation of proteins serves to mark them for degradation by the 26 S proteasome. Protein ubiquitylation is achieved by a multistep mechanism involving several enzymes: a ubiquitin-activating enzyme (E1), a ubiquitin-conjugating enzyme (E2), and a ubiquitin-protein ligase (E3). A new class of ubiquitylation enzymes, the ubiquitin chain assembly factor (E4), was recently discovered and shown to be required for the degradation of certain types of substrate, including an artificial fusion protein with an $NH_2$-terminal ubiquitin moiety, via a ubiquitin fusion degradation pathway (7, 8). *Saccharomyces cerevisiae* Ufd2, the prototype E4 enzyme, binds to the oligoubiquitylated artificial ubiquitin fusion degradation substrate and catalyzes extension of the ubiquitin chain. We previously identified E4B (also known as UFD2a) as a mammalian ortholog of yeast Ufd2. E4B contains the conserved U-box domain at its COOH terminus, and this domain mediates the interaction of E4B with ubiquitin-conjugated targets. The U-box domain appears to be an essential functional domain for E4 activity (9, 10). E4B is expressed predominantly in neuronal tissues of adult mice (10) and has thus been suggested to play a biological role in the nervous system. Indeed, $E4B^{+/-}$ mice manifest axonal dystrophy in the nucleus gracilis as well as degeneration of Purkinje cells associated with endoplasmic reticulum stress, and develop a neurological disorder (11).

Neurodegenerative diseases including Parkinson disease, Alzheimer disease, as well as polyglutamine diseases such as

* This work was supported in part by a grant from the Ministry of Education, Culture, Sports, Science, and Technology of Japan and by a research grant from the Takeda Science Foundation.

[S] The on-line version of this article (available at http://www.jbc.org) contains supplemental Figs. S1 and S2.

[1] To whom correspondence should be addressed: Dept. of Molecular and Cellular Biology, Medical Institute of Bioregulation, Kyushu University, 3-1-1 Maidashi, Higashi-ku, Fukuoka, Fukuoka 812-8582, Japan. Tel.: 81-92-642-6815; Fax: 81-92-642-6819; E-mail: nakayak1@bioreg.kyushu-u.ac.jp.

[2] The abbreviations used are: POMC, pro-opiomelanocortin; PVN, paraventricular nucleus; BAT, brown adipose tissue; WAT, white adipose tissue; UCP1, uncoupling protein 1; α-MSH, α-melanocyte-stimulating hormone; WT, wild-type; Tg, transgenic.

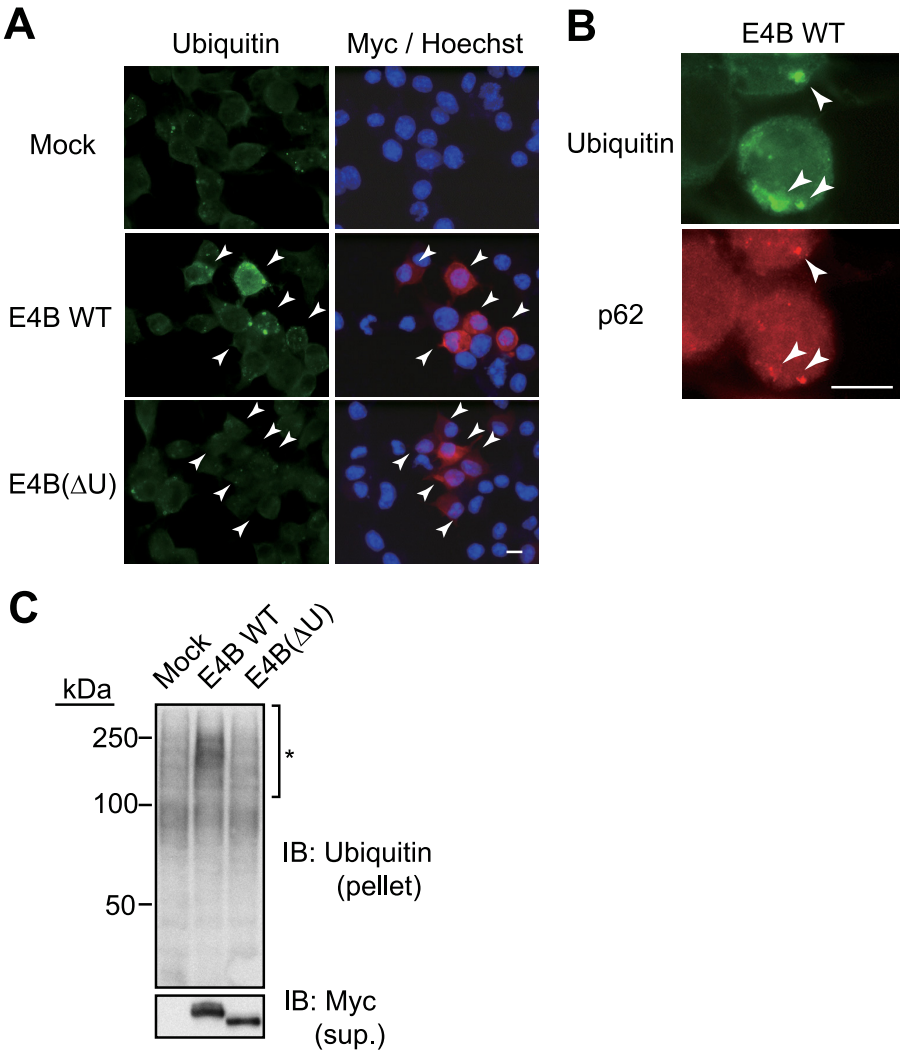


FIGURE 1. **Accumulation of ubiquitin- and p62-positive aggregates induced by forced expression of E4B in cultured cells.** *A*, Neuro2A cells were transfected with expression vectors encoding Myc epitope-tagged wild-type (*WT*) or ΔU mutant forms of E4B, or with the corresponding empty vector (*Mock*), for 24 h, after which the cells were subjected to immunofluorescence analysis with antibodies to polyubiquitin (*green*) and the Myc epitope (*red*). Nuclei were stained with Hoechst 33258 (*blue*). *Arrowheads* indicate cells expressing ectopic E4B. *Scale bar*, 10 μm. *B*, Neuro2A cells transfected with the expression vector for Myc epitope-tagged WT E4B as in *A* were subjected to immunofluorescence analysis with antibodies to polyubiquitin (*green*) and p62 (*red*). *Arrowheads* indicate cellular aggregates stained by both types of antibodies. *Scale bar*, 10 μm. *C*, Neuro2A cells transfected as in *A* were lysed in radioimmunoprecipitation assay buffer, the lysates were centrifuged at 20,000 × *g* for 15 min at 4 °C, and the resulting pellet and supernatant (*sup.*) were subjected to immunoblot (*IB*) analysis with antibodies to polyubiquitin or the Myc epitope, respectively. *Asterisk* indicates ubiquitin conjugates of high molecular weight.

Huntington disease and spinocerebellar ataxias are characterized by the formation of intracellular protein aggregates in neurons and neuronal loss. These diseases have been linked to the ubiquitin-proteasome system by the observation that the intracellular aggregates are recognized by antibodies to ubiquitin. Furthermore, several ubiquitylation enzymes including E4B have been implicated in the pathogenesis of such diseases (12–18). The multifunctional adaptor protein p62, which contains domains that mediate protein-protein interaction, was also recently shown to associate with the ubiquitin-positive aggregates and promote their formation (19–23). This protein is thus now used as a marker for cellular ubiquitin aggregates.

Several studies have suggested the existence of a link between neurodegenerative diseases and obesity. Obesity and associated metabolic disorders induced by genetic mutations or diet thus appear to promote neural degeneration in animals and humans (24). Conversely, certain hereditary neurodegenerative diseases in humans are associated with obesity or diabetes (25). These findings suggest that neurodegeneration in certain brain regions might be responsible for obesity in some individuals. However, a causal relationship between neural degeneration and obesity has not been demonstrated experimentally to date.

We have now established an animal model of obesity that is induced by neural degeneration. We found that forced expression of E4B in cultured cells resulted in heterotopic accumulation of ubiquitin- and p62-positive aggregates similar to those associated with neurodegenerative diseases. Aggregate formation was also observed in hypothalamic neurons responsible for regulation of food intake and energy expenditure in E4B transgenic mice. It was accompanied by degeneration and functional impairment of these neurons, resulting in the development of hyperphagic obesity and other metabolic abnormalities. The E4B transgenic mouse model thus appears to recapitulate the pathological features both of neurodegenerative diseases as well as of obesity and related metabolic disorders, indicating the existence of a direct link between these conditions.

## EXPERIMENTAL PROCEDURES

*Cell Culture, Construction of Expression Plasmids, and Cell Transfection*—Neuro2A cells were cultured in Dulbecco's modified Eagle's medium supplemented with fetal bovine serum (10%), sodium pyruvate (1 mM), L-glutamine (2 mM), 2-mercaptoethanol (50 μM), non-essential amino acids (10 ml/liter), penicillin (100 units/ml), and streptomycin (100 mg/ml). The cDNAs for mouse E4B or its E4B(ΔU) mutant (26) tagged with the Myc epitope at their $NH_2$ termini were subcloned into pcDNA3 (Invitrogen), and the resulting vectors were introduced into Neuro2A cells with the use of the Lipofectamine 2000 reagent (Invitrogen). The formation of ubiquitin-positive aggregates was observed at a low level in cells exposed to the transfection reagent alone, but the formation of such aggregates was greatly increased by overexpression of E4B. Cells for immunoblot analysis of polyubiquitin

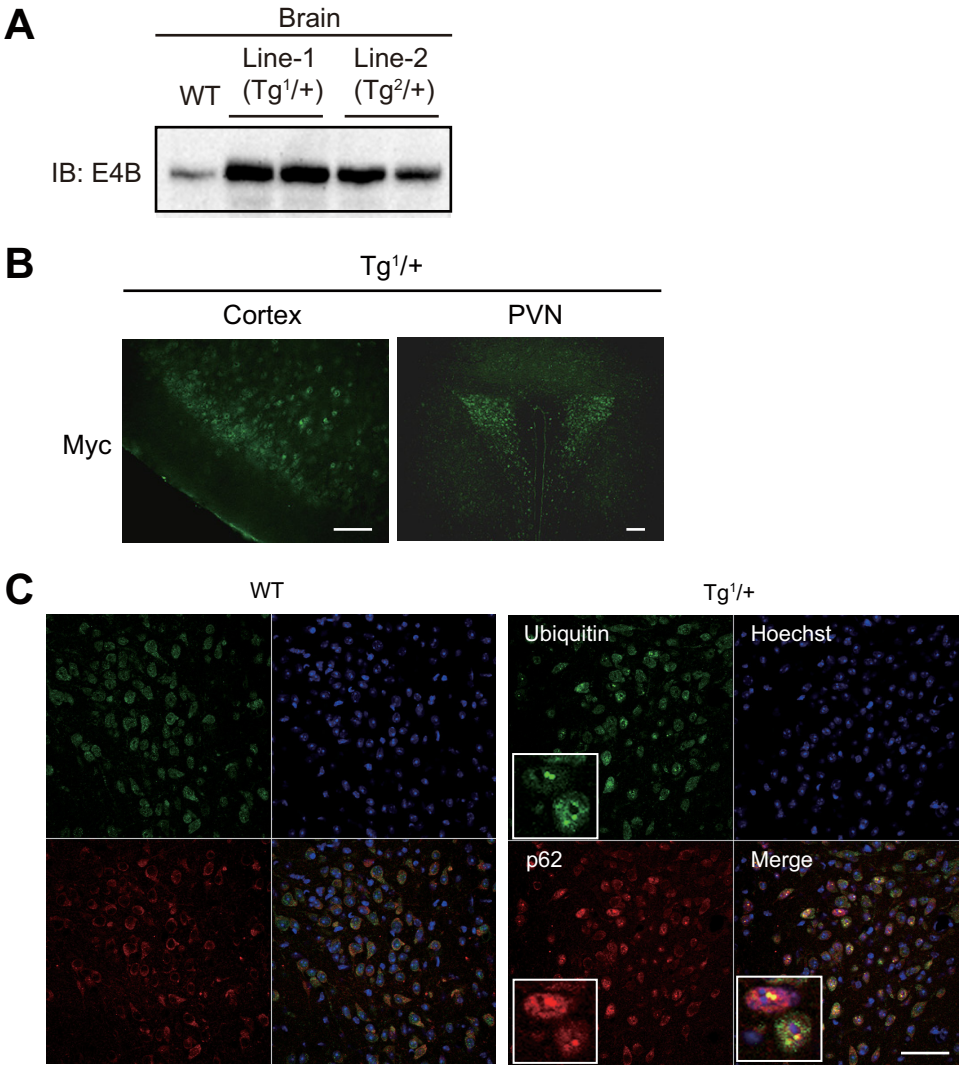


FIGURE 2. **Accumulation of ubiquitin- and p62-positive aggregates in hypothalamic nuclei of E4B transgenic mice.** *A*, the brain of WT or E4B transgenic mice harboring one allele of the transgene (line 1, $Tg^1/+$ or line 2, $Tg^2/+$) was lysed with RIPA buffer and then subjected to immunoblot (*IB*) analysis with antibodies to E4B. *B*, immunofluorescence analysis of the brain of $Tg^1/+$ mice with antibodies to the Myc epitope. Representative images of the cerebral cortex and the hypothalamic PVN are shown. *Scale bars*, 100 $\mu$m. *C*, confocal immunofluorescence microscopy of the PVN region of 4-month-old WT or $Tg^1/+$ mice with antibodies to polyubiquitin (*green*) and p62 (*red*). Nuclei were stained with Hoechst 33258 (*blue*). *Insets* show higher magnification views of portions of the main images. *Scale bars*, 50 $\mu$m.

were cultured at 33 °C overnight before transfection to further facilitate aggregate formation.

*Histological Analysis and Sample Preparation for Immunofluorescence Analysis of the Brain*—The inguinal fat pad (as WAT), BAT, and liver were fixed with 4% paraformaldehyde and embedded in paraffin. Sections (thickness, 4 $\mu$m) of WAT and BAT were stained with hematoxylin-eosin. The brain was fixed by perfusion with 4% paraformaldehyde and subjected to postfixation for at most 3 days. After fixation, the liver and brain were infiltrated with 25% (w/v) sucrose in 0.1 M phosphate buffer for at least 2 days, and frozen sections (thickness, 30 to 40 $\mu$m) were prepared with a sliding microtome (Yamato Kohki Industrial, Saitama, Japan). Sections of the liver were stained with oil red O (Nacalai tesque, Kyoto, Japan), and floating sections of the brain were subjected to immunofluorescence analysis.

*Immunoblot and Immunofluorescence Analyses*—Immunoblot and immunofluorescence analyses of cultured cells or the brain were performed as described previously with some optimization (27). Immunoblots were probed with antibodies to the Myc epitope (9E10, Sigma), polyubiquitin (FK2; Nippon Biotest Laboratories, Tokyo, Japan), E4B (BD Transduction Laboratories), or Hsp70 (BD Transduction Laboratories). Immunofluorescence analysis of both cultured cells and brain sections was performed with antibodies to the Myc epitope (9E10), polyubiquitin (FK2), p62 (28), glial fibrillary acidic protein (Cy3-conjugated, Sigma), or c-Fos (Calbiochem). Nuclei were stained with Hoechst 33258. Specimens were observed with a fluorescence microscope (Nikon) or a confocal microscope (LSM510, Carl Zeiss).

*Animal Experiments*—Animal experiments were performed in accordance with the guidelines of Kyushu University. For generation of transgenic mouse lines, cDNAs for mouse E4B or E4B(ΔU) (26) tagged with the Myc epitope at their $NH_2$ termini were subcloned into the XhoI site of the pPrPpE1/E2,E3sal plasmid (29). The resulting vectors were digested with NotI for linearization and removal of the backbone vector. The prepared DNA constructs were then injected into fertilized eggs of the B6D2F1/Crlj (BDF1) background. Primary genotyping was performed by PCR and Southern blot analysis followed by immunoblot analysis with antibodies to the Myc epitope. Examination of phenotypes was performed with C57BL/6J × DBA/2 background mice because E4B transgenic mice on the C57BL/6J background were sterile for some unknown reason. Wild-type (WT) littermates were used as control mice. For the leptin tolerance test, individually housed mice deprived of food for 12 h were injected (intraperitoneal) with recombinant mouse leptin (30 mg/kg of body weight; R&D Systems) or vehicle, and food intake was determined over the subsequent 12-h period. CT scanning and calculation of the percentage of body fat were performed as described previously (30). For determination of paraventricular nucleus (PVN) neuron activity, an indwelling cannula was implanted into the left lateral ventricle (0.2 mm posterior, 0.95 mm left of the bregma, 1.5 to 1.6 mm below the surface of the skull) of 4-week-old mice anesthetized with pentobarbital (55–60 mg/kg, intraperitoneal). One week

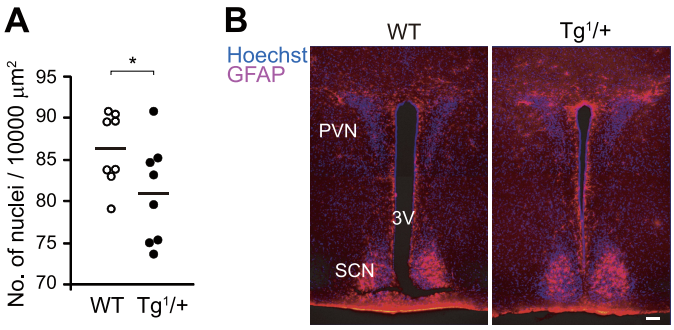


FIGURE 3. **Neural degeneration and gliosis in the hypothalamic PVN of E4B transgenic mice.** *A*, brain sections of 9- to 10-month-old WT or $Tg^1/+$ mice were stained with Hoechst 33258 and observed with a confocal microscope. The area of the PVN was calculated by accessory software, and the density of cell nuclei in this area (*right* and *left regions* of the PVN from four mice of each genotype) was determined. Data are shown as a dot plot with the means indicated by *horizontal lines* (*, $p < 0.05$, one-tailed Student's *t* test). *B*, immunofluorescence analysis of the PVN region of 10-week-old WT or $Tg^1/+$ mice with antibodies to glial fibrillary acidic protein (*GFAP*) (*red*). Nuclei were stained with Hoechst 33258 (*blue* fluorescence). *SCN* and *3V* indicate the suprachaismatic nucleus and third ventricle, respectively. *Scale bar,* 100 μm.

later, 2 μl of either α-melanocyte-stimulating hormone (α-MSH) (2 μg/μl; Peptide Institute, Osaka, Japan) or saline vehicle were injected through the cannula at a rate of 3 μl/min. The animals were killed and subjected to perfusion fixation at 1 h after injection of α-MSH or vehicle, and serial sections of the PVN were prepared and subjected to immunofluorescence staining for c-Fos. All images were collected at the same exposure time, and a pair of images of the PVN of WT and transgenic mice with the strongest c-Fos signals was selected for further analysis. The intensity of the c-Fos signal at each soma in the PVN region was calculated with Photoshop software (Adobe). Serum leptin concentration (fasted condition) as well as serum insulin, adiponectin, triglyceride, and total cholesterol concentrations (fed condition) were determined as described previously (31). The glucose tolerance test and insulin tolerance test were also performed as described previously with some modifications (30).

*Quantitative Reverse Transcription-PCR Analysis*—Total RNA (1 μg) isolated from the hypothalamus or BAT with the use of Isogen (Wako) was subjected to reverse transcription with the use of a Quantitect Kit (Qiagen). The resulting cDNA was subjected to real-time PCR analysis as described previously (32). The amount of each target mRNA was normalized by the corresponding amount of glyceraldehyde-3-phosphate dehydrogenase mRNA, and the normalized values were then expressed relative to that for WT mice. The PCR primers (forward and reverse, respectively) were as follows: 5′-TACCAAGCTGTGCGATGT-3′ and 5′-AAGCCCAATGATGTTCAGT-3′ for *Ucp1*; 5′-CTTTGGCGGAGGTGCTAGA-3′ and 5′-GGACTCGTGCAGCCTTACACA-3′ for agouti-related protein; 5′-CTACTCCGCTCTGCGACACT-3′ and 5′-AGTGTCTCAGGGCTGGATCTC-3′ for neuropeptide Y; and 5′-AACATCTTTGTCCCCAGAGAGCT-3′ and 5′-AGCAGAATCTCGGCATCTTCC-3′ for *Pomc*.

*Statistical Analysis*—Quantitative data are presented as mean ± S.D. unless indicated otherwise and were analyzed by Student's *t* test (two-tailed unless indicated otherwise) or the Mann-Whitney *U* test as performed with Excel or R software, respectively. A *p* value of $<0.05$ was considered statistically significant.

## RESULTS

*Intracellular Aggregate Formation Induced by Expression of E4B*—We introduced a vector encoding Myc epitope-tagged WT E4B or an E4B mutant that lacks the U-box domain (ΔU) into mouse neuronal cell line Neuro2A. Immunofluorescence analysis with antibodies to polyubiquitin and the Myc epitope tag revealed the formation of ubiquitin-positive aggregates in a part of cells expressing WT E4B, whereas few such aggregates were detected in cells expressing E4B(ΔU) or in mock transfected cells (Fig. 1*A*). The aggregates were also reactive with antibodies to p62 (Fig. 1*B*), an adaptor protein that was recently shown to associate with ubiquitin-positive aggregates (19, 22). Consistent with these observations, immunoblot analysis with antibodies to polyubiquitin revealed that the intensity of the slow-migrating smear corresponding to polyubiquitin conjugates was greater in the pellet fraction of cells expressing WT E4B than in that of E4B(ΔU)-expressing or mock transfected cells (Fig. 1*C*). These results thus suggested that elongation of ubiquitin chains resulting from increased E4B activity leads to the formation of ubiquitin- and p62-positive intracellular aggregates.

*Aggregate Formation and Neural Degeneration in Hypothalamic Nuclei of E4B Transgenic Mice*—To investigate whether the E4B-induced formation of intracellular aggregates was reproducible in neural cells in the brain, we generated mice transgenic for a Myc epitope-tagged E4B construct controlled by the promoter of the gene for the mammalian prion promoter (29). Neuron-specific transgene expression in regions of the brain in which endogenous E4B is also expressed (data not shown) was confirmed by immunoblot (Fig. 2*A*) and immunohistofluorescence (Fig. 2*B*) analyses. Among the generated transgenic mouse lines, animals of line 1 harboring one allele of the transgene ($Tg^1/+$) were used for most of the examinations described below because of their higher level of transgene expression (Fig. 2*A*). As observed in cultured cells, ubiquitin- and p62-positive aggregates were detected in a subset of hypothalamic neurons of $Tg^1/+$ mice including those of the PVN (Fig. 2*C*), dorsomedial hypothalamic nucleus, arcuate nucleus, and lateral hypothalamus, but such aggregates were not apparent in the cerebral cortex (supplemental Fig. S1). These aggregates were formed particularly in hypothalamic neurons that expressed the transgene at high levels (supplemental Fig. S2), as was also observed in cultured Neuro2A cells (Fig. 1*A*). Ectopic E4B was not localized to the aggregates (supplemental Fig. S2), however, excluding the possibility that overexpression of E4B resulted in the aggregation of E4B itself.

Similar formation of aggregates by aggregation-prone toxic proteins is associated with neural cell death in neurodegenerative diseases such as Alzheimer and Huntington (33). We therefore investigated whether aggregate formation in E4B transgenic mice is also associated with neural degeneration. The number of cell nuclei in the PVN region was found to be decreased in aged $Tg^1/+$ mice compared with that in WT animals (Fig. 3*A*). The number of glial fibrillary acidic protein-positive glial cells was also increased around the PVN region

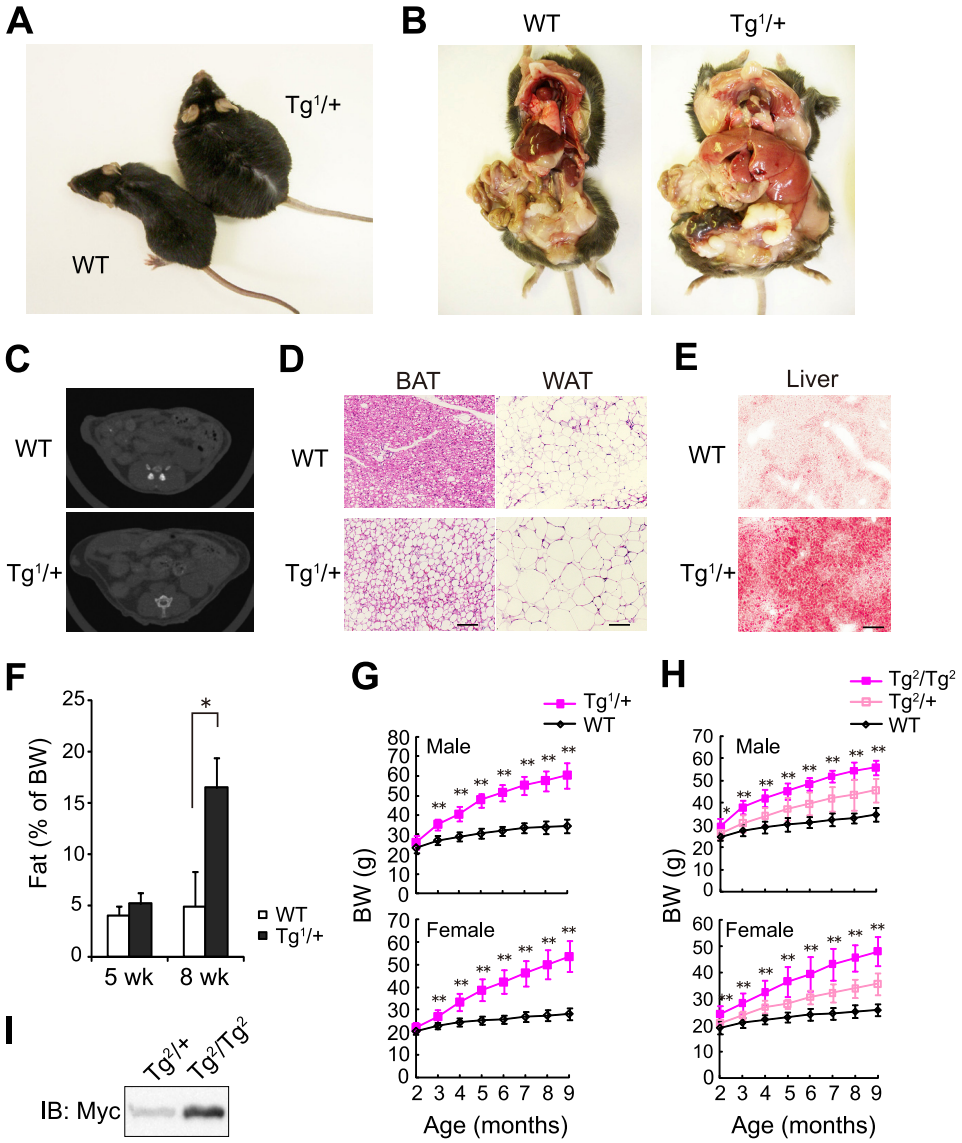


FIGURE 4. **Development of obesity in E4B transgenic mice on a normal diet.** *A–C*, gross appearance (*A*), anatomy (*B*), and CT scans of the abdomen (*C*) of 9-month-old $Tg^1/+$ and WT littermates. *D* and *E*, hematoxylin-eosin staining of white (*WAT*) or brown (*BAT*) adipose tissue (*D*) as well as oil red O staining of the liver (*E*) of 6–7-month-old $Tg^1/+$ and WT littermates. *Scale bars*, 100 $\mu$m in *D* or 200 $\mu$m in *E*. *F*, body fat as a percentage of body weight for WT ($n = 3$) or $Tg^1/+$ mice ($n = 3–4$) at 5 and 8 weeks of age. *Error bars* represent ± S.D. (*, $p < 0.05$, Student's *t* test). *G* and *H*, time course of body weight for WT ($n = 6–8$), $Tg^1/+$ ($n = 7–8$), $Tg^2/+$ ($n = 6–7$) or $Tg^2/Tg^2$ mice ($n = 4–7$). *Error bars* represent ± S.D. (*, $p < 0.05$; **, $p < 0.01$ for WT *versus* $Tg^1/+$ (*G*) or $Tg^2/Tg^2$ (*H*) animals, Student's *t* test). *I*, immunoblot (*IB*) analysis with antibodies to the Myc epitope for brain lysates prepared with RIPA buffer from $Tg^2/+$ or $Tg^2/Tg^2$ mice.

of $Tg^1/+$ mice (Fig. 3*B*). Together, these observations were indicative of neural cell death and gliosis in the transgenic animals. Neural degeneration was thus associated with the formation of ubiquitin-positive aggregates in hypothalamic neurons (especially, PVN neurons) of $Tg^1/+$ mice.

*Development of Obesity in E4B Transgenic Mice*—The hypothalamus functions as the center for regulation of food intake and energy expenditure. In particular, the PVN has long been identified as a satiety center, given that lesions within the PVN result in the development of hyperphagic obesity (34). Given that the formation of ubiquitin-positive aggregates and associated neural degeneration were observed in the hypothalamus of E4B transgenic mice, we examined whether these animals might exhibit dysregulation of food intake and energy expenditure leading to obesity. Indeed, $Tg^1/+$ mice were unequivocally obese (Fig. 4*A*) and manifested increased lipid accumulation in subcutaneous and visceral adipose tissue as well as the liver (Fig. 4*B*). Excessive lipid accumulation was also apparent in CT images (Fig. 4*C*) as well as in tissue sections of WAT or BAT (Fig. 4*D*) and the liver (Fig. 4*E*). The body weight of $Tg^1/+$ mice was increased at 2 to 3 months of age compared with that of WT mice, and this increase was preceded by an increase in the amount of body fat apparent at 8 weeks of age (Fig. 4, *F* and *G*). An increase in body weight was also observed in another E4B transgenic line ($Tg^2/+$), excluding the possibility that the phenotype was artifactual or the result of unintended gene disruption rather than the effect of transgene expression (Fig. 4*H*). The expression level of the transgene in $Tg^2/+$ was lower than those of line 1 (Fig. 2*A*), and the extent of obesity in $Tg^2/+$ animals was about half of that in those of line 1 (Fig. 4, *G* and *H*). In addition, the extent of obesity in line 2 animals harboring two alleles of the transgene ($Tg^2/Tg^2$) was about twice that in littermates harboring only one allele (Fig. 4, *H* and *I*) and was similar to that in mice of $Tg^1/+$ harboring only one allele (Fig. 4*G*). These observations thus indicated that the obese phenotype is directly related to the expression level of the transgene. The body weight of $Tg^1/+$ mice or $Tg^2/Tg^2$ mice at 9 months of age was about twice that of age-matched WT animals (Fig. 4, *G* and *H*).

*Dependence of E4B Transgenic Mouse Phenotypes on Ubiquitylation Activity*—To examine whether the phenotypes of E4B transgenic mice are dependent on the ubiquitylation activity of E4B, we generated transgenic mice that express Myc epitope-tagged E4B(ΔU) under control of the same prion gene promoter as that used for expression of the WT protein. Because the comparable expression level of the E4B(ΔU) transgene to the WT E4B transgene of $Tg^1/+$ mice were achieved in mice harboring two alleles of the E4B(ΔU) transgene ($Tg^{\Delta U}/Tg^{\Delta U}$) (Fig. 5*A*), these mice were used for most examinations and comparisons described below. No aggregates positive for polyubiquitin and p62 were detected in the hypothalamus of $Tg^{\Delta U}/Tg^{\Delta U}$ mice (Fig. 5*B*). Furthermore, $Tg^{\Delta U}/Tg^{\Delta U}$ mice did not differ substantially from WT animals in terms of body weight (Fig.

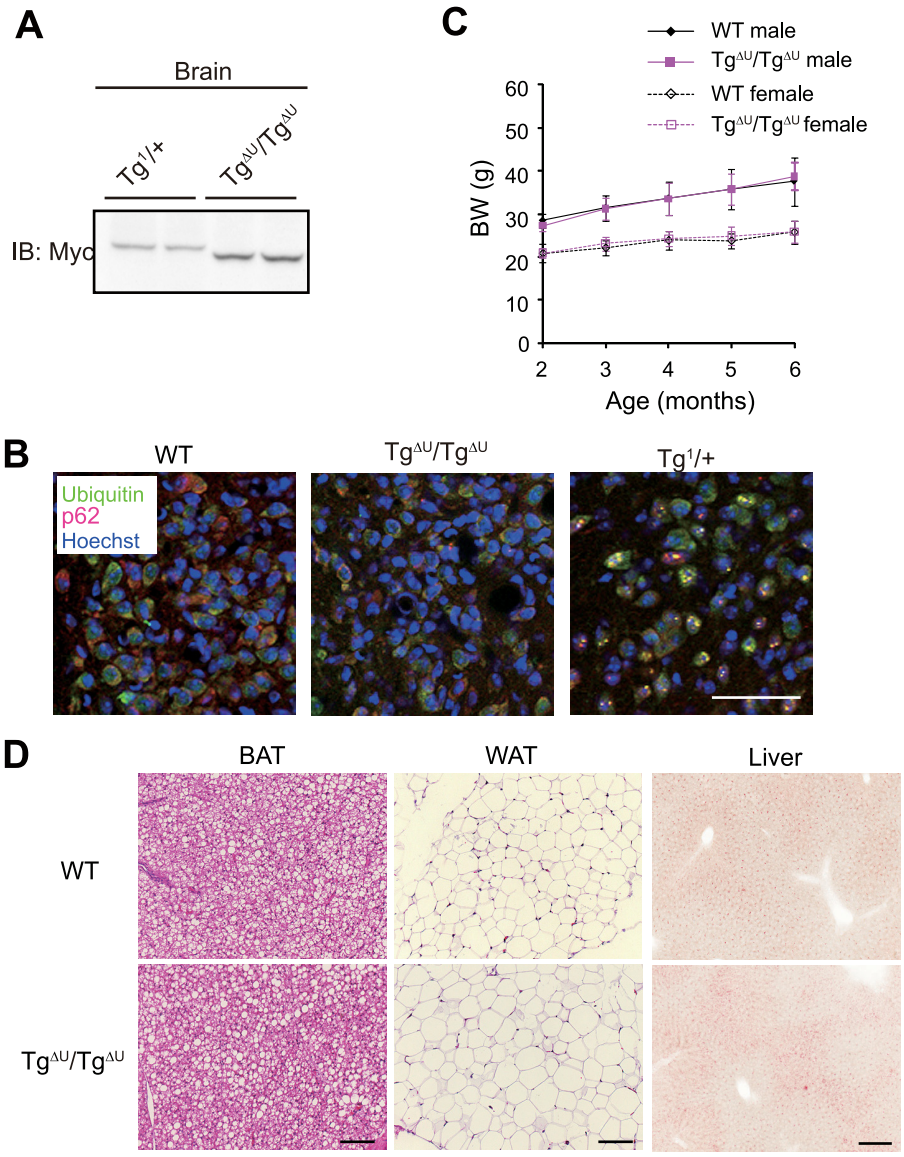


FIGURE 5. **Phenotypes of E4B(ΔU) transgenic mice.** *A*, the brain of $Tg^1/+$ mice or E4B(ΔU) transgenic mice harboring two alleles of the transgene ($Tg^{\Delta U}/Tg^{\Delta U}$) mice was lysed with RIPA buffer and subjected to immunoblot (*IB*) analysis with antibodies to the Myc epitope. *B*, immunofluorescence analysis of the PVN region of 6-month-old WT or $Tg^{\Delta U}/Tg^{\Delta U}$ mice or a 4-month-old $Tg^1/+$ mouse was performed as described in the legend to Fig. 2*C*. *Scale bar*, 50 μm. *C*, time course of body weight for WT ($n = 5$) or $Tg^{\Delta U}/Tg^{\Delta U}$ mice ($n = 6$). *Error bars* represent ± S.D. (no significant difference). *D*, hematoxylin-eosin staining of BAT or WAT as well as oil red O staining of the liver of 6-month-old WT or $Tg^{\Delta U}/Tg^{\Delta U}$ mice. *Scale bars*, 100 (BAT and WAT) or 200 μm (liver).

5*C*) or the extent of lipid accumulation in adipose tissue or liver (Fig. 5*D*). These results were also confirmed with another $Tg^{\Delta U}/Tg^{\Delta U}$ line (data not shown). These results thus indicated that the obese phenotype of E4B transgenic mice is largely dependent on the increased enzymatic activity of E4B.

*Association of Obesity in E4B Transgenic Mice with Functional Impairment of the Hypothalamic Satiety Center*—We next examined whether the obese phenotype of E4B transgenic mice is attributable to malfunction of the hypothalamic satiety center that regulates food intake and energy expenditure. Compared with WT mice, $Tg^1/+$ mice showed an increase in food intake that was apparent as early as 5 weeks of age (Fig. 6*A*), before the development of leptin resistance (see Fig. 7*A*) and obesity (Fig. 4*G*). We estimated energy expenditure by monitoring expression of the gene for uncoupling protein 1 (*Ucp1*), an essential mediator of heat production in BAT. Expression of the *Ucp1* gene in BAT was previously shown to be controlled by the action of several hypothalamic neuropeptides (35–41). The amount of *Ucp1* mRNA in BAT of $Tg^1/+$ mice tended to be decreased at 5 weeks of age and was significantly decreased at 8 weeks of age compared with WT mice (Fig. 6*B*). These results suggested that the regulation of food intake and energy expenditure was impaired in E4B transgenic mice prior to development of the obese phenotype.

Leptin is an adipocyte-derived satiety factor that acts on a subset of neurons in the hypothalamus and thereby regulates food intake and energy expenditure (2, 42). Hyperphagia associated with impaired hypothalamic function is attributable, at least in part, to a reduced response of hypothalamic neurons to leptin. We therefore next performed a leptin tolerance test to examine leptin sensitivity in $Tg^1/+$ mice. Whereas injection (intraperitoneal) of leptin inhibited food intake in WT mice, it had no effect on that in $Tg^1/+$ mice at 5 weeks of age (Fig. 6*C*), supporting the notion that the hypothalamus of the transgenic animals is functionally impaired. Furthermore, the amounts of mRNAs for the hypothalamic orexigenic neuropeptides agouti-related protein and neuropeptide Y in the fasted condition were significantly decreased in $Tg^1/+$ mice at 5 weeks of age compared with WT mice (Fig. 6*D*). These neuropeptides antagonize anorexigenic signals mediated by POMC neurons (2–4), but the abundance of *Pomc* mRNA in the hypothalamus did not differ between WT and $Tg^1/+$ mice (Fig. 6*D*), suggesting that the altered expression of the orexigenic neuropeptide genes was not attributable to a primary loss of POMC neurons but was rather likely due to defects in secondary neurons in the feeding circuit, such as PVN neurons. We investigated the activity of PVN neurons evoked by intracerebroventricular injection of α-MSH, a proteolytic product of POMC that activates PVN neurons mainly by binding to melanocortin receptor 4 and regulates food intake (43–46). The activity of PVN neurons was monitored by immunostaining of c-Fos, an immediate-early gene product expressed in response to neural stimulation. Whereas the activity of PVN neurons was markedly in-

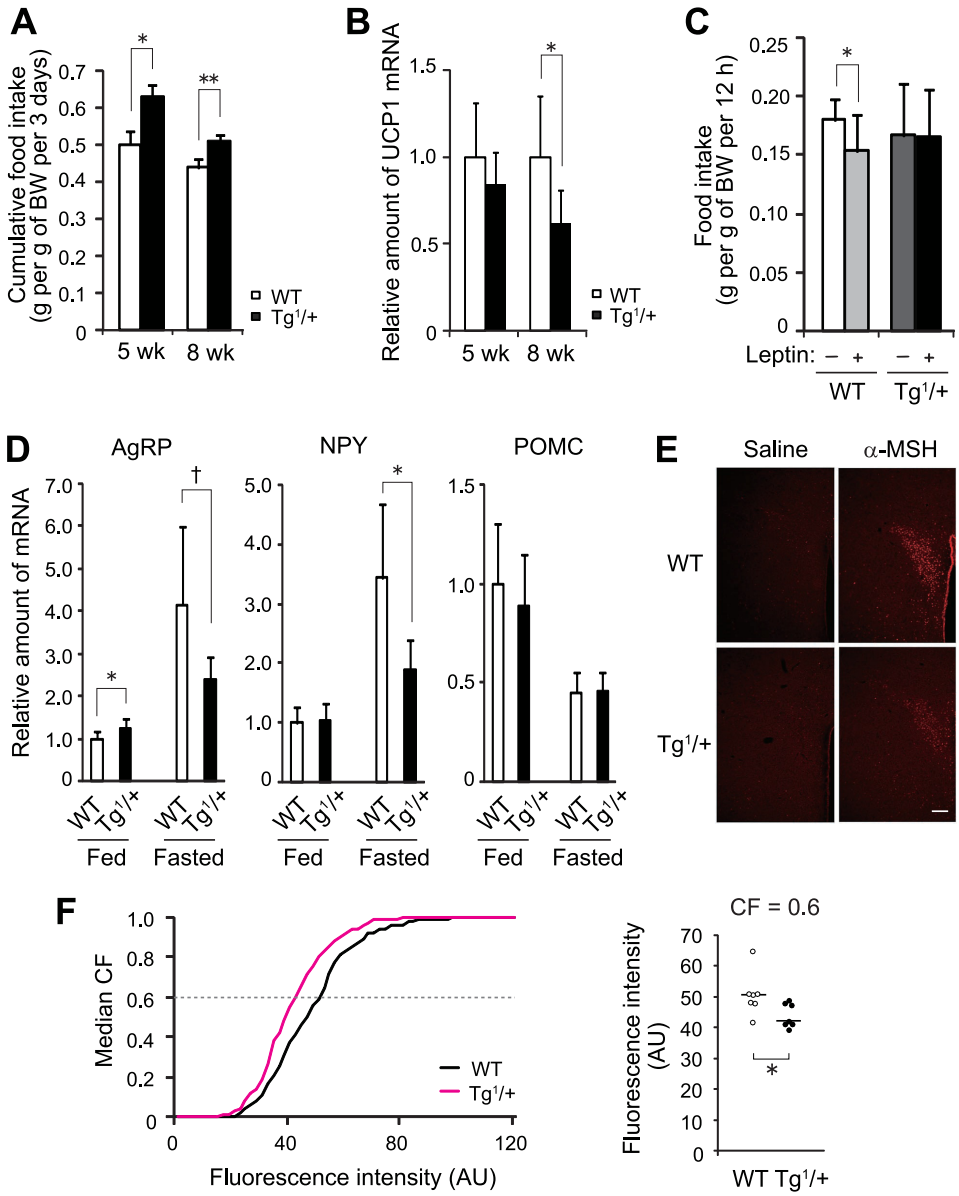


FIGURE 6. **Functional impairment of the hypothalamic satiety center in E4B transgenic mice.** *A*, cumulative food intake over 3 days for WT ($n = 8$) or Tg$^1$/+ mice ($n = 4$) at 5 and 8 weeks of age. *Error bars* represent ± S.D. (*, $p < 0.05$; **, $p < 0.01$, Student's *t* test). *B*, quantitative reverse transcription-PCR analysis of *Ucp1* mRNA in BAT of 5- or 8-week-old WT or Tg$^1$/+ mice ($n = 9$ in each group). Normalized data are expressed relative to the corresponding value for WT mice, and are mean ± S.D. (*, $p < 0.05$, Student's *t* test). *C*, leptin tolerance test for 5-week-old WT ($n = 9$–10) or Tg$^1$/+ mice ($n = 9$). *Error bars* represent ± S.D. (*, $p < 0.05$, Student's *t* test). *D*, quantitative reverse transcription-PCR analysis of agouti-related protein (*AgRP*), neuropeptide Y (*NPY*), and *Pomc* mRNAs in the hypothalamus of 5-week-old WT ($n = 5$–6) or Tg$^1$/+ mice ($n = 6$–7) in the fed or fasted (for 48 h) conditions. Normalized data are expressed relative to the corresponding value for fed WT mice, and are mean ± S.D. (*, $p < 0.05$, two-tailed Student's *t* test; †, $p < 0.05$, one-tailed Student's *t* test). *E*, immunofluorescence analysis with antibodies to c-Fos for the PVN of 5-week-old WT or Tg$^1$/+ mice at 1 h after intracerebroventricular injection of vehicle (saline) or α-MSH. *Scale bar*, 100 μm. *F*, quantitative analysis of c-Fos signals in images similar to those in *E*. The median of the cumulative frequency (*CF*) of fluorescence intensity at each soma in the PVN ($n = 7$ in each genotype) is shown in the *left panel*. The *dotted line* indicates a threshold (CF = 0.6) for the comparison of fluorescence intensity between individual animals of the two genotypes shown in the *right panel*. The *horizontal lines* in the *right panel* indicate medians (*, $p = 0.0175$, Mann-Whitney *U* test).

creased by intracerebroventricular injection of α-MSH in WT mice, this effect was greatly attenuated in Tg$^1$/+ mice (Fig. 6, *E* and *F*). Together, these results indicated that the responsiveness of PVN neurons to anorexigenic stimuli is reduced in E4B transgenic mice as a result of neuronal organic disorders, and that consequent functional impairment of the satiety center leads to increased food intake, reduced energy expenditure, and obesity.

*Obesity-associated Metabolic Disorders in E4B Transgenic Mice*—We finally investigated obesity-associated disorders in E4B transgenic mice. Monitoring serum leptin concentration revealed the presence of hyperleptinemia in Tg$^1$/+ mice as early as 6 weeks of age (Fig. 7*A*), suggesting the development of leptin resistance at the age before the increase in body weight and fat mass at 2 to 3 months of age (Fig. 4, *F* and *G*). We further examined whether E4B transgenic mice manifested glucose intolerance and insulin resistance associated with obesity. To this end, we performed a glucose tolerance test and insulin tolerance test at 2 or 9 months of age. Two-month-old Tg$^1$/+ mice, which do not differ from their WT littermates in body weight (Fig. 4*G*), exhibited normal glucose tolerance and did not manifest insulin resistance (Fig. 7*B*). In contrast, 9-month-old Tg$^1$/+ mice, which are markedly obese (Fig. 4*G*), exhibited significant glucose intolerance and insulin resistance (Fig. 7*B*), indicating that the transgenic animals develop type 2 diabetes mellitus in association with obesity. Consistent with these observations, whereas 2-month-old Tg$^1$/+ mice exhibited only slight hyperinsulinemia, this condition had deteriorated substantially by 9 months of age (Table 1), indicative of the progression of obesity-associated insulin resistance. In addition, Tg$^1$/+ mice manifested significant hypercholesterolemia and hypoadiponectinemia (Table 1). These findings thus revealed that E4B transgenic mice develop many of the characteristics associated with human obesity, suggesting that these animals represent a new model for the study of obesity and metabolic disorders induced by neurodegeneration.

## DISCUSSION

We have shown that an increased abundance and activity of E4B result in the formation of intracellular aggregates positive for both ubiquitin and p62. The formation of such

aggregates in the brain leads to degeneration and functional impairment of a subset of hypothalamic neurons that are responsible for the regulation of food intake and energy expenditure and the consequent development of hyperphagic obesity. Collectively, our results obtained with E4B transgenic mice shed light on the physiological link between neurodegeneration and obesity, providing new opportunities for the study of the mechanism and treatment of obesity and its related disorders in humans.

Obesity and its associated metabolic abnormalities have become a worldwide public health problem, and new well defined animal models for obesity research are urgently needed. We now propose that E4B transgenic mice possess several advantages as such a model. First, these animals spontaneously develop obesity and thus do not need to be fed a high-fat diet. Second, they manifest abnormalities in the highly restricted area of the hypothalamic satiety center and thus exhibit pathological features similar to those of some other mouse models of obesity such as *ob*/*ob* and *db*/*db* mice in which hypothalamic leptin circuit is impaired (42, 47). Third, only one allele of the E4B transgene is required for mice to develop obesity. Furthermore, the extent of obesity can be varied by selection of transgenic lines with different levels of expression or different numbers of alleles of the transgene, whereas most other mouse models are loss-of-function mutants and therefore require homozygosity of the mutant allele for manifestation of the phenotype. And finally, E4B transgenic mice develop leptin and insulin resistance, glucose intolerance, hypercholesterolemia, and hypoadiponectinemia during progression of the obesity phenotype, indicating that these animals recapitulate the course of human obesity. In addition to providing support for the usefulness of E4B transgenic mice as a model for human obesity, our findings suggest the possibility that aberrant activity of E4B might be a cause of this condition in humans, a notion that is also consistent with the localization of obesity-related genetic markers in the vicinity of the *Ueb4b* (the gene symbol for E4B) gene locus (48, 49).

Our results also indicate that E4B transgenic mice are a useful model for investigations into the more general physiological relevance of intracellular aggregate formation. Dysfunction of the ubiquitin-proteasome system has been implicated in the pathogenesis of various neurodegenerative diseases including Alzheimer, Parkinson, and polyglutamine diseases such as Huntington, given that the intracellular deposits of aggregated proteins associated with these conditions have been shown to contain ubiquitin conjugates. Although the toxicity of these deposits and their relevance to disease pathogenesis remain controversial, their formation appears to result in part from an

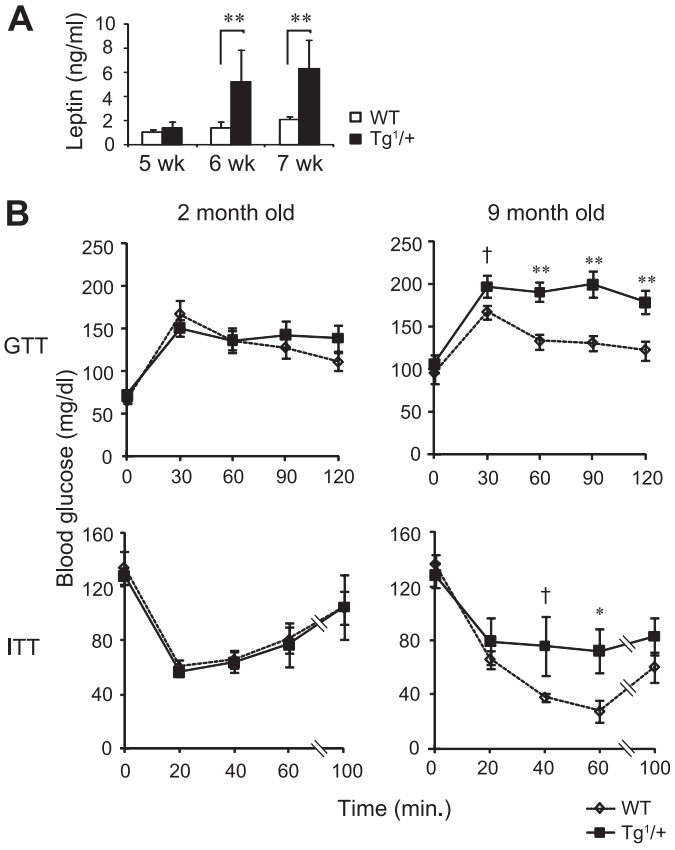


FIGURE 7. **Obesity-associated metabolic disorders in E4B transgenic mice.** *A*, serum concentration of leptin in WT ($n = 5–6$) or Tg$^1$/+ mice ($n = 5–7$) at 5, 6, or 7 weeks of age after the animals had been deprived of food for at least 12 h. *Error bars* represent ± S.D. (**, $p < 0.01$, Student's *t* test). *B*, glucose tolerance test (*GTT*) and insulin tolerance test (*ITT*) for WT ($n = 6–8$) or Tg$^1$/+ mice ($n = 6–8$) at 2 or 9 months of age. *Error bars* represent ± S.D. (*, $p < 0.05$; **, $p < 0.01$, two-tailed Student's *t* test; †, $p < 0.05$, one-tailed Student's *t* test) *versus* the corresponding WT value.

**TABLE 1**

**Serum analysis of Tg$^1$/+ and WT mice**

Serum concentration of triglyceride, total cholesterol, insulin, and adiponectin in WT or Tg$^1$/+ mice at 2 or 9 months of age are shown. Hypercholesterolemia, hyperinsulinemia, and hypoadiponectinemia, all of which are metabolic abnormalities associated with obesity, had deteriorated substantially by 9 months of age of Tg$^1$/+ mice. Upper and lower values of each pair are from WT and Tg$^1$/+ mice, respectively.

| Analyte | Triglyceride | Total cholesterol | Insulin | Adiponectin |
|---|---|---|---|---|
| | *mg/dl* | | *ng/ml* | *μg/ml* |
| **2-Month-old males** | | | | |
| WT ($n = 5–6$) | 93.47 ± 23.98 | 87.88 ± 6.23 | 0.80 ± 0.31 | 1.75 ± 0.087 |
| Tg$^1$/+ ($n = 8$) | 110.78 ± 27.53 | 108.85 ± 15.67[a] | 3.43 ± 2.32[b] | 2.48 ± 0.76[b] |
| **2-Month-old females** | | | | |
| WT ($n = 6$) | 67.13 ± 29.18 | 60.47 ± 8.57 | 1.95 ± 2.17 | 2.43 ± 0.55 |
| Tg$^1$/+ ($n = 8$) | 59.85 ± 24.50 | 79.19 ± 8.05[a] | 1.72 ± 0.78[b] | 3.47 ± 0.59[a] |
| **9-Month-old males** | | | | |
| WT ($n = 6–7$) | 174.56 ± 45.63 | 86.44 ± 11.82 | 3.47 ± 2.04 | 2.44 ± 0.40 |
| Tg$^1$/+ ($n = 6–8$) | 214.26 ± 48.10 | 154.51 ± 56.89[a] | 25.51 ± 12.36[a] | 1.74 ± 0.55[b] |
| **9-Month-old females** | | | | |
| WT ($n = 6–7$) | 228.11 ± 97.55 | 66.90 ± 21.60 | 1.00 ± 0.48 | 4.58 ± 1.21 |
| Tg$^1$/+ ($n = 7$) | 243.31 ± 131.49 | 108.41 ± 35.62[b] | 7.22 ± 6.40[b] | 4.29 ± 1.08 |

[a] Data are mean ± S.D., $p < 0.01$, *versus* the corresponding value for WT mice using the Student's *t* test.
[b] Data are mean ± S.D., $p < 0.05$, *versus* the corresponding value for WT mice using the Student's *t* test.

impairment of a ubiquitin-proteasome system flux (50–67) that is attributable to several factors including the accumulation of ubiquitin-conjugated proteins to an extent that exceeds the capacity of the proteasome, retention of proteasome components in the aggregates, and inhibition of substrate delivery by aggregate-associated p62 (61, 68–74). Similar aggregates have been observed in tissues or cells including neurons with defects in autophagy, another pathway for the clearance of cellular components (19, 75). We have now shown that increased activity of E4B also induced intracellular aggregate formation in cultured cells or neurons in the brain. Although the mechanism of aggregate formation induced by excess E4B activity remains to be elucidated, there are several possibilities. First, the E4B-mediated elongation of ubiquitin chains attached to physiological substrates might inhibit the degradation of these proteins by the proteasome. Appropriate pruning of ubiquitin chains is necessary for recognition of substrates by the proteasome, and the balance between chain elongation and pruning might be shifted by excess E4B activity. Second, substrates that are not ubiquitylated in the presence of normal levels of E4B might become ubiquitylated in the presence of excess E4B, and the resulting ubiquitylated proteins might be prone to form intracellular aggregates. Although we have not identified the ubiquitylated components of the E4B-induced aggregates, our observation that aggregate formation was restricted to a limited area of the hypothalamus in the brain, a feature not apparent in most other models of neurodegenerative diseases, is suggestive of the presence of a specific E4B substrate in the hypothalamic neurons. So far, few proteins were shown to have properties of forming aggregates in hypothalamic neurons. One such protein is poly(A)-binding protein nuclear 1 (PABPN1), which was shown to form filamentous structures in neurosecretory neurons of the hypothalamus (76). We thus speculate that such aggregate-prone protein(s) may be involved in the process. Alternatively, it is also possible that overexpressed E4B aberrantly activates a specific E3–E4 ubiquitylation pathway only in the hypothalamus, resulting in ubiquitylation of proteins expressing broadly in the brain. If it is the case, proteins involved in other neurodegenerative diseases, such as Tau, $\alpha$-synuclein, and Huntingtin, might be targeted by the E4B-dependent ubiquitylation in the hypothalamus, given that the aggregates seen in E4B transgenic mice resemble those in other neurodegenerative diseases.

Most studies of the relationship between obesity and neurodegeneration in animal models or humans have focused on the possibility that obesity and related metabolic disorders exacerbate neurodegeneration and thereby promote cognitive decline and increase vulnerability to brain injury (24). Few studies have addressed the possibility that neurodegeneration in the brain may cause obesity, as is suggested by hereditary neurodegenerative disorders associated with obesity such as Prader-Willi syndrome (25). Our genetic mouse model has provided the first experimental demonstration that neurodegeneration can indeed result in obesity, suggesting that some cases of human obesity might be attributable to hypothalamic neurodegeneration.

In conclusion, we have shown that increased activity of the mammalian E4 pathway results in the accumulation of intracellular aggregates both in cultured cells and in a subset of hypothalamic neurons in the brain that are responsible for regulation of food intake and energy expenditure. The formation of these aggregates in hypothalamic neurons resulted in associated structural and functional abnormalities as well as the development of hyperphagic obesity. Our E4B transgenic mice have thus revealed a physiological link between the pathogenesis of neurodegenerative diseases and obesity.

*Acknowledgments—We thank M. Nakazato, H. Yamaguchi, K. Toshinai, and T. Matsuo for technical advice; T. Ishii for kindly providing anti-p62; Y. Yamada, K. Takeda, M. Tanaka, N. Kitajima, and S. Yamamura for technical assistance; and A. Ohta and N. Kimura for help in preparation of the manuscript.*

## REFERENCES

1. Casper, R. C., Sullivan, E. L., and Tecott, L. (2008) *Psychopharmacology* **199,** 313–329
2. Schwartz, M. W., Woods, S. C., Porte, D., Jr., Seeley, R. J., and Baskin, D. G. (2000) *Nature* **404,** 661–671
3. Jobst, E. E., Enriori, P. J., and Cowley, M. A. (2004) *Trends Endocrinol. Metab.* **15,** 488–499
4. Cone, R. D. (2005) *Nat. Neurosci.* **8,** 571–578
5. Hershko, A., and Ciechanover, A. (1998) *Annu. Rev. Biochem.* **67,** 425–479
6. Pickart, C. M. (2001) *Annu. Rev. Biochem.* **70,** 503–533
7. Johnson, E. S., Ma, P. C., Ota, I. M., and Varshavsky, A. (1995) *J. Biol. Chem.* **270,** 17442–17456
8. Koegl, M., Hoppe, T., Schlenker, S., Ulrich, H. D., Mayer, T. U., and Jentsch, S. (1999) *Cell* **96,** 635–644
9. Hatakeyama, S., Yada, M., Matsumoto, M., Ishida, N., and Nakayama, K. I. (2001) *J. Biol. Chem.* **276,** 33111–33120
10. Kaneko, C., Hatakeyama, S., Matsumoto, M., Yada, M., Nakayama, K., and Nakayama, K. I. (2003) *Biochem. Biophys. Res. Commun.* **300,** 297–304
11. Kaneko-Oshikawa, C., Nakagawa, T., Yamada, M., Yoshikawa, H., Matsumoto, M., Yada, M., Hatakeyama, S., Nakayama, K., and Nakayama, K. I. (2005) *Mol. Cell. Biol.* **25,** 10953–10964
12. Ciechanover, A., and Brundin, P. (2003) *Neuron* **40,** 427–446
13. Petrucelli, L., Dickson, D., Kehoe, K., Taylor, J., Snyder, H., Grover, A., De Lucia, M., McGowan, E., Lewis, J., Prihar, G., Kim, J., Dillmann, W. H., Browne, S. E., Hall, A., Voellmy, R., Tsuboi, Y., Dawson, T. M., Wolozin, B., Hardy, J., and Hutton, M. (2004) *Hum. Mol. Genet.* **13,** 703–714
14. Shimura, H., Schwartz, D., Gygi, S. P., and Kosik, K. S. (2004) *J. Biol. Chem.* **279,** 4869–4876
15. Imai, Y., Soda, M., Inoue, H., Hattori, N., Mizuno, Y., and Takahashi, R. (2001) *Cell* **105,** 891–902
16. Imai, Y., Soda, M., Hatakeyama, S., Akagi, T., Hashikawa, T., Nakayama, K. I., and Takahashi, R. (2002) *Mol. Cell* **10,** 55–67
17. Chung, K. K., Zhang, Y., Lim, K. L., Tanaka, Y., Huang, H., Gao, J., Ross, C. A., Dawson, V. L., and Dawson, T. M. (2001) *Nat. Med.* **7,** 1144–1150
18. Matsumoto, M., Yada, M., Hatakeyama, S., Ishimoto, H., Tanimura, T., Tsuji, S., Kakizuka, A., Kitagawa, M., and Nakayama, K. I. (2004) *EMBO J.* **23,** 659–669
19. Komatsu, M., Waguri, S., Koike, M., Sou, Y. S., Ueno, T., Hara, T., Mizushima, N., Iwata, J., Ezaki, J., Murata, S., Hamazaki, J., Nishito, Y., Iemura, S., Natsume, T., Yanagawa, T., Uwayama, J., Warabi, E., Yoshida, H., Ishii, T., Kobayashi, A., Yamamoto, M., Yue, Z., Uchiyama, Y., Kominami, E., and Tanaka, K. (2007) *Cell* **131,** 1149–1163
20. Nagaoka, U., Kim, K., Jana, N. R., Doi, H., Maruyama, M., Mitsui, K., Oyama, F., and Nukina, N. (2004) *J. Neurochem.* **91,** 57–68
21. Gal, J., Ström, A. L., Kilty, R., Zhang, F., and Zhu, H. (2007) *J. Biol. Chem.* **282,** 11068–11077
22. Zatloukal, K., Stumptner, C., Fuchsbichler, A., Heid, H., Schnoelzer, M., Kenner, L., Kleinert, R., Prinz, M., Aguzzi, A., and Denk, H. (2002) *Am. J. Pathol.* **160,** 255–263

23. Nezis, I. P., Simonsen, A., Sagona, A. P., Finley, K., Gaumer, S., Contamine, D., Rusten, T. E., Stenmark, H., and Brech, A. (2008) *J. Cell Biol.* **180,** 1065–1071
24. Bruce-Keller, A. J., Keller, J. N., and Morrison, C. D. (2009) *Biochim. Biophys. Acta* **1792,** 395–400
25. Ristow, M. (2004) *J. Mol. Med.* **82,** 510–529
26. Okumura, F., Hatakeyama, S., Matsumoto, M., Kamura, T., and Nakayama, K. I. (2004) *J. Biol. Chem.* **279,** 53533–53543
27. Ishida, N., Hara, T., Kamura, T., Yoshida, M., Nakayama, K., and Nakayama, K. I. (2002) *J. Biol. Chem.* **277,** 14355–14358
28. Ishii, T., Yanagawa, T., Kawane, T., Yuki, K., Seita, J., Yoshida, H., and Bannai, S. (1996) *Biochem. Biophys. Res. Commun.* **226,** 456–460
29. Borchelt, D. R., Davis, J., Fischer, M., Lee, M. K., Slunt, H. H., Ratovitsky, T., Regard, J., Copeland, N. G., Jenkins, N. A., Sisodia, S. S., and Price, D. L. (1996) *Genet. Anal.* **13,** 159–163
30. Oike, Y., Akao, M., Yasunaga, K., Yamauchi, T., Morisada, T., Ito, Y., Urano, T., Kimura, Y., Kubota, Y., Maekawa, H., Miyamoto, T., Miyata, K., Matsumoto, S., Sakai, J., Nakagata, N., Takeya, M., Koseki, H., Ogawa, Y., Kadowaki, T., and Suda, T. (2005) *Nat. Med.* **11,** 400–408
31. Ishigaki, Y., Katagiri, H., Yamada, T., Ogihara, T., Imai, J., Uno, K., Hasegawa, Y., Gao, J., Ishihara, H., Shimosegawa, T., Sakoda, H., Asano, T., and Oka, Y. (2005) *Diabetes* **54,** 322–332
32. Susaki, E., Nakayama, K., Yamasaki, L., and Nakayama, K. I. (2009) *Proc. Natl. Acad. Sci. U.S.A.* **106,** 5192–5197
33. Taylor, J. P., Hardy, J., and Fischbeck, K. H. (2002) *Science* **296,** 1991–1995
34. Leibowitz, S. F., Hammer, N. J., and Chang, K. (1981) *Physiol. Behav.* **27,** 1031–1040
35. Wang, C., Billington, C. J., Levine, A. S., and Kotz, C. M. (2000) *Neuroreport* **11,** 3251–3255
36. Masaki, T., Chiba, S., Yoshimichi, G., Yasuda, T., Noguchi, H., Kakuma, T., Sakata, T., and Yoshimatsu, H. (2003) *Endocrinology* **144,** 2741–2748
37. Masaki, T., Yoshimichi, G., Chiba, S., Yasuda, T., Noguchi, H., Kakuma, T., Sakata, T., and Yoshimatsu, H. (2003) *Endocrinology* **144,** 3547–3554
38. Yasuda, T., Masaki, T., Kakuma, T., and Yoshimatsu, H. (2003) *Neurosci. Lett.* **349,** 75–78
39. Scarpace, P. J., and Matheny, M. (1998) *Am. J. Physiol.* **275,** E259–E264
40. Baran, K., Preston, E., Wilks, D., Cooney, G. J., Kraegen, E. W., and Sainsbury, A. (2002) *Diabetes* **51,** 152–158
41. Small, C. J., Kim, M. S., Stanley, S. A., Mitchell, J. R., Murphy, K., Morgan, D. G., Ghatei, M. A., and Bloom, S. R. (2001) *Diabetes* **50,** 248–254
42. Friedman, J. M., and Halaas, J. L. (1998) *Nature* **395,** 763–770
43. Sarkar, S., Légrádi, G., and Lechan, R. M. (2002) *Brain Res.* **945,** 50–59
44. Kim, M. S., Rossi, M., Abusnana, S., Sunter, D., Morgan, D. G., Small, C. J., Edwards, C. M., Heath, M. M., Stanley, S. A., Seal, L. J., Bhatti, J. R., Smith, D. M., Ghatei, M. A., and Bloom, S. R. (2000) *Diabetes* **49,** 177–182
45. Wirth, M. M., Olszewski, P. K., Yu, C., Levine, A. S., and Giraudo, S. Q. (2001) *Peptides* **22,** 129–134
46. Kublaoui, B. M., Holder, J. L., Jr., Gemelli, T., and Zinn, A. R. (2006) *Mol. Endocrinol.* **20,** 2483–2492
47. Elmquist, J. K., Elias, C. F., and Saper, C. B. (1999) *Neuron* **22,** 221–232
48. Stone, S., Abkevich, V., Hunt, S. C., Gutin, A., Russell, D. L., Neff, C. D., Riley, R., Frech, G. C., Hensel, C. H., Jammulapati, S., Potter, J., Sexton, D., Tran, T., Gibbs, D., Iliev, D., Gress, R., Bloomquist, B., Amatruda, J., Rae, P. M., Adams, T. D., Skolnick, M. H., and Shattuck, D. (2002) *Am. J. Hum. Genet.* **70,** 1459–1468
49. Deng, H. W., Deng, H., Liu, Y. J., Liu, Y. Z., Xu, F. H., Shen, H., Conway, T., Li, J. L., Huang, Q. Y., Davies, K. M., and Recker, R. R. (2002) *Am. J. Hum. Genet.* **70,** 1138–1151
50. Bence, N. F., Sampat, R. M., and Kopito, R. R. (2001) *Science* **292,** 1552–1555
51. López Salon, M., Morelli, L., Castaño, E. M., Soto, E. F., and Pasquini, J. M. (2000) *J. Neurosci. Res.* **62,** 302–310
52. Lopez Salon, M., Pasquini, L., Besio Moreno, M., Pasquini, J. M., and Soto, E. (2003) *Exp. Neurol.* **180,** 131–143
53. Keller, J. N., Hanni, K. B., and Markesbery, W. R. (2000) *J. Neurochem.* **75,** 436–439
54. Almeida, C. G., Takahashi, R. H., and Gouras, G. K. (2006) *J. Neurosci.* **26,** 4277–4288
55. Oh, S., Hong, H. S., Hwang, E., Sim, H. J., Lee, W., Shin, S. J., and Mook-Jung, I. (2005) *Mech. Ageing Dev.* **126,** 1292–1299
56. Tseng, B. P., Green, K. N., Chan, J. L., Blurton-Jones, M., and LaFerla, F. M. (2008) *Neurobiol. Aging* **29,** 1607–1618
57. Song, S., Kim, S. Y., Hong, Y. M., Jo, D. G., Lee, J. Y., Shim, S. M., Chung, C. W., Seo, S. J., Yoo, Y. J., Koh, J. Y., Lee, M. C., Yates, A. J., Ichijo, H., and Jung, Y. K. (2003) *Mol. Cell* **12,** 553–563
58. McNaught, K. S., and Jenner, P. (2001) *Neurosci. Lett.* **297,** 191–194
59. Bennett, E. J., Bence, N. F., Jayakumar, R., and Kopito, R. R. (2005) *Mol. Cell* **17,** 351–365
60. Bennett, E. J., Shaler, T. A., Woodman, B., Ryu, K. Y., Zaitseva, T. S., Becker, C. H., Bates, G. P., Schulman, H., and Kopito, R. R. (2007) *Nature* **448,** 704–708
61. Jana, N. R., Zemskov, E. A., Wang, Gh., and Nukina, N. (2001) *Hum. Mol. Genet.* **10,** 1049–1059
62. Seo, H., Sonntag, K. C., and Isacson, O. (2004) *Ann. Neurol.* **56,** 319–328
63. Petrucelli, L., O'Farrell, C., Lockhart, P. J., Baptista, M., Kehoe, K., Vink, L., Choi, P., Wolozin, B., Farrer, M., Hardy, J., and Cookson, M. R. (2002) *Neuron* **36,** 1007–1019
64. Wang, J., Wang, C. E., Orr, A., Tydlacka, S., Li, S. H., and Li, X. J. (2008) *J. Cell Biol.* **180,** 1177–1189
65. Stefanis, L., Larsen, K. E., Rideout, H. J., Sulzer, D., and Greene, L. A. (2001) *J. Neurosci.* **21,** 9549–9560
66. Tanaka, Y., Engelender, S., Igarashi, S., Rao, R. K., Wanner, T., Tanzi, R. E., Sawa, A. L., Dawson, V., Dawson, T. M., and Ross, C. A. (2001) *Hum. Mol. Genet.* **10,** 919–926
67. Keck, S., Nitsch, R., Grune, T., and Ullrich, O. (2003) *J. Neurochem.* **85,** 115–122
68. Esser, C., Alberti, S., and Höhfeld, J. (2004) *Biochim. Biophys. Acta* **1695,** 171–188
69. Kwak, S., Masaki, T., Ishiura, S., and Sugita, H. (1991) *Neurosci. Lett.* **128,** 21–24
70. Cummings, C. J., Mancini, M. A., Antalffy, B., DeFranco, D. B., Orr, H. T., and Zoghbi, H. Y. (1998) *Nat. Genet.* **19,** 148–154
71. Wigley, W. C., Fabunmi, R. P., Lee, M. G., Marino, C. R., Muallem, S., DeMartino, G. N., and Thomas, P. J. (1999) *J. Cell Biol.* **145,** 481–490
72. García-Mata, R., Bebök, Z., Sorscher, E. J., and Sztul, E. S. (1999) *J. Cell Biol.* **146,** 1239–1254
73. Waelter, S., Boeddrich, A., Lurz, R., Scherzinger, E., Lueder, G., Lehrach, H., and Wanker, E. E. (2001) *Mol. Biol. Cell* **12,** 1393–1407
74. Korolchuk, V. I., Mansilla, A., Menzies, F. M., and Rubinsztein, D. C. (2009) *Mol. Cell* **33,** 517–527
75. Hara, T., Nakamura, K., Matsui, M., Yamamoto, A., Nakahara, Y., Suzuki-Migishima, R., Yokoyama, M., Mishima, K., Saito, I., Okano, H., and Mizushima, N. (2006) *Nature* **441,** 885–889
76. Berciano, M. T., Villagra, N. T., Ojeda, J. L., Navascues, J., Gomes, A., Lafarga, M., and Carmo-Fonseca, M. (2004) *Hum. Mol. Genet.* **13,** 829–838